

# Beamforming for 5G Cellular Communications with Analyzing the Linear and Circular Polarized Antenna Arrays Gain Effect

Amany M. Saleh<sup>1, \*</sup>, Mahmoud M. Elmesalawy<sup>1</sup>,  
Korany R. Mahmoud<sup>1, 2</sup>, and Ibrahim I. Ibrahim<sup>1</sup>

**Abstract**—Since massive multiple-input multiple-output (MIMO) array and beamforming significantly improve spectrum efficiency, where beamforming adapts the radiation pattern of the massive array, most previous studies focus on the MIMO beamforming optimization problem to maximize the utility of the system by assuming that a massive array consists of an isotropic antenna. This research work was conducted to investigate the beamforming optimization problem with practical elements in a MIMO array. By inserting the effect of a practical antenna array gain in the channel model, the impact of array elements feeding on the beamforming optimization problem could be illustrated. Furthermore, the beamforming optimization, non-convex issue, is reformulated to synonymous convex optimization issue, through a weighted minimum mean square error (WMMSE) technique. Consequently, a conformal array (CfA) with a half wavelength dipole element is proposed at the base station (BS). The simulation results display that the suggested WMMSE-beamforming technique performance with considering antenna array gain effect can yield much better and accurate system performance than the other algorithms. Eventually, to analyze the impact of array gain on the optimization problem solution in addition to boot the network capacity, a curl antenna array in octagonal prism geometry is created. The curl antenna is circularly polarized and has a high gain compared to the half-wavelength dipole.

## 1. INTRODUCTION

The fifth-generation (5G) cellular communication systems have been assisted by technologies that produce significant improvements in cell throughput. Massive multiple-input multiple-output (MIMO), where a base station (BS) utilizing a huge number of antennas simultaneously serves many users using the same time-frequency resource, is one of the major technologies for a 5G system [1–4]. The antenna array enables an increase in the capacity of the wireless system by successfully reducing multipath fading and channel interference. This will be realized by concentrating signal radiation only in the anticipated direction and modifying such radiation according to the signal surroundings or traffic situations using beamforming techniques. In wireless systems, receiving and transmitting beamforming is applied to signal transmission from BSs with multiple antennas to one or multiple pieces of user equipment that should be covered. The objective of transmit beamforming is to maximize each user's received signal power while minimizing the interference signal power from the other users, hence increasing capacity. This can be achieved by transmitting the same signal from all transmitters with different amplitudes and phases. These multiple versions of the transmitted signal will pass through different MIMO channels, such that they are added constructively to the desirable users and destructively to other users [5–8]. Therefore, massive MIMO systems combined with beamforming antenna array technologies are expected to play a key role in 5G wireless systems. Based on the literature review, several studies have been

---

*Received 22 February 2022, Accepted 17 March 2022, Scheduled 7 April 2022*

\* Corresponding author: Amany M. Saleh (amany\_mohamed\_saleh@h-eng.helwan.edu.eg).

<sup>1</sup> Electronics and Communications Department, Faculty of Engineering, Helwan University, Cairo 11795, Egypt. <sup>2</sup> National Telecommunications Regulatory Authority, Giza 12577, Egypt.

applied on how to optimize the receive and/or transmit beamforming vectors optimization with different constraints. Some objective functions of the optimization problem are treated in this research, like system utility maximization and minimization of system transmission BS power. In [9], the authors use the weighted minimum mean square error (WMMSE) technique to settle the system rate maximization issue under the transmitted power of per-BS constrain with the splitting of the beamforming process between the receiver and transmitter to raise the design simplicity of the user receiver. Furthermore, a beamforming algorithm dependent on a group of three separate steps is proposed in [10] to settle the issue of how to minimize the system power under two constraints: the receiver SINR and each BS transmitted power. The WMMSE technique is applied in [11] to settle the system rate maximization issue with two constraints, each on the BS transmitted power and capacity of the backhaul. This WMMSE process is also utilized in [12] to procure an optimal settlement to minimize joint energy and resource allocation problems with respect to the time task it takes to execute, transmit power, data rates of the fronthaul, and computation capacity constraints.

The group-sparse optimization and the programming algorithms based on relaxed-integer are used to optimize total energy minimization problem with three constraints which are downlink SINR for each user, each BS transmitted power, and the power from each user [13]. The robust beamforming approach is suggested for the total power minimization issue with threshold per-user mean square error (MSE) [14]. Li et al. in [15] present the issue of how to maximize the total network utility under quality of service (QoS) requirements, backhaul capacity, and load constraints. All these previous works did not reflect the impact of antenna array geometry on the system performance. Therefore, [16, 17] consider planar array (PA) geometry and uniform linear array (ULA) geometry per BS. But all these researches still did not consolidate the per-antenna power which is a significant restraint in MIMO array network practical realization. Therefore, a multiuser downlink MIMO system is used to investigate the issue of receiving and transmitting beamforming vectors optimization to maximize the overall system achievable rate. This optimization issue has been solved under some constraints like users' QoS, the transmitted power from each antenna, and total BS transmitted power. Furthermore, the impact of various array geometries made up of isotropic antenna elements arranged at BS has been investigated [18]. On the other hand, in [19] the authors strive to find the optimum solution of the downlink rate problem for a single-cell massive MIMO system concerning the antennas number and power variables in the BS with overall power and QoS requirements constraints. In [20, 21], the authors demonstrate that when an array of various antenna elements is used, there is a significant difference in the gain radiation pattern. This difference in gain pattern is produced by mutual coupling, edge effect, arrival angle, and the geometry of the array. So, in this research, the massive MIMO channel model is modified with the impact of practical antenna array gain. In addition, the received and transmitted beamformer optimization problems are studied in a multiuser downlink MIMO system to maximize the system total rate with users' QoS, transmitted power by each antenna, and total transmitted power by BS constraints. Finally, the curl antenna is designed at 2.6 GHz to investigate the impact of antenna gain on system execution, where the curl antenna has a higher gain than an ideal dipole antenna. Moreover, the curl antenna, a circularly polarised antenna, is used to increase the system capacity. The following contributions are particularly noteworthy:

- (i) The channel model is modified to consider the practical antenna array gain.
- (ii) Half-wavelength dipole elements that make up the conformal array geometry are suggested to be structured at BS to decrease the interference inside the cell and concentrate the BS power towards the specified users with high directivity, narrow beamwidth, and null of the level of side lobes.
- (iii) A WMMSE procedure is suggested to settle the optimization issue of the transmitting and receiving beamforming vectors. The link between the system total rate maximization issue and the weighted MSE minimization issue is utilized to convert the constrained non-convex optimization issue into a convex one.
- (iv) The viability of the suggested array geometry gain variation on the suggested settlement to calculate the receive and transmit beamforming vectors in addition to its relative performance based on the previous work in [18] will be illustrated numerically. Specifically, conformal array (CfA) geometry with the suggested settlement outperformed the previous solution in [18] concerning consumed power by the system and overall system throughput.

- (v) For more improvement in intra-cell interference between the users, another practical antenna array element is designed and studied. This antenna array element is a curl antenna where this antenna is a circularly polarized one. Therefore, finally, the possibility of dividing the users' parts into those which receive vertically and others which connect horizontally with the BS is designed to raise the system capacity.

This research is organized as follows. The system model is displayed in the second section. Section 3 introduces the design of the CfA geometry with two different antenna array elements and its steering vectors. The problem formulation is produced in Section 4. Section 5 produces a settlement for calculating the receiving and transmitting MIMO array beamforming vectors. Numerical results, in addition to its discussions, are given in Section 6. Section 7 presents the conclusions.

The following notations are utilized throughout the paper. Lowercase bold letters are used for vectors. However, upper bold letters are used for matrices.  $(\cdot)$  represents element by element matrix multiplications.  $\mathbb{R}+$  represents positive real domain. Furthermore,  $\mathbb{C}$  is used for the complex domain. The notation  $\|\cdot\|^2$  is used for the vector two-norm, while  $(\cdot)^H$  and  $(\cdot)^{-1}$  refer to matrix conjugate transpose and inverse of the matrix, respectively.  $E[\cdot]$  notation refers to the expectation matrix and  $I$  for the identity matrix.  $[\cdot]_{\varepsilon,\varepsilon}$  is used for the matrix  $(\varepsilon,\varepsilon)$  entry.  $|\cdot|$  for both scalar absolute value and the set cardinality, based on the situation. The scalar imaginary part and real part are represented as  $\text{Im}(\cdot)$  and  $\text{Re}(\cdot)$ , respectively.

## 2. SYSTEM MODEL

Assume a multiuser downlink MIMO system comprising  $k$  users and a single BS as displayed in Fig. 1. In this model, each user requires a specific QoS concerning the needed SINR. The BS consists of  $N_t$  transmitting antennas; however, all users have a single antenna. The all users index set is represented as  $\mathcal{S} = \{1, 2, \dots, k\}$  with cardinality  $k$ . The transmitted beamforming vector is  $\mathbf{w}_k \in \mathbb{C}^{N_t \times 1}$  that is used by BS to transmit  $x_k \in \mathbb{C}$  with  $\{E[|x_k|^2] = 1\}$  which is the data symbol to  $k^{th}$  user, assuming that BS transmits a single stream of data. The BS has been considered to transmit data streams that are independent of their connected users simultaneously using the same frequency unit. The received signal to user  $k$  from BS is expressed as follows.

$$\mathbf{y}_k = \mathbf{H}_k \cdot \mathbf{H}_k^{\text{ant}} \mathbf{w}_k x_k + \sum_{i \neq k, i \in \mathcal{S}} \mathbf{H}_k \cdot \mathbf{H}_k^{\text{ant}} \mathbf{w}_i x_i + \mathbf{n}_k \tag{1}$$

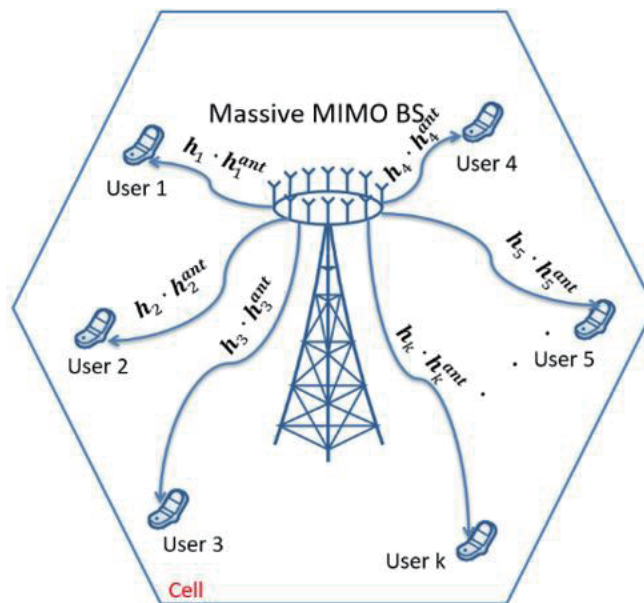


Figure 1. Downlink multiuser massive MIMO system model.

where  $\mathbf{y}_k \in \mathbb{C}^{N_r \times 1}$  is the received signal vector at user  $K$ ;  $\mathbf{H}_k \in \mathbb{C}^{N_r \times N_t}$  represents the channel matrix between user  $k$  and BS;  $\mathbf{H}_k^{\text{ant}}$  is the channel matrix of antenna array; and  $n_k \in \mathbb{C}^{N_r \times 1}$  is the additive white Gaussian noise which has a mean equal to zero and variance  $\sigma^2 \mathbf{I}$ . The second part of Eq. (1) denotes the downlink interference inside the cell. The user  $k$  estimated symbol  $\hat{x}_k$  at its receiver can be as [18]:

$$\hat{x}_k = \mathbf{u}_k^H \mathbf{y}_k \quad (2)$$

where  $\mathbf{u}_k \in \mathbb{C}^{N_r \times 1}$  is the vector of received beamforming at user  $k$ . The downlink received signal to interference and noise ratio (SINR) at user  $k$  can be represented as follows:

$$\text{SINR}_k = \frac{|\mathbf{u}_k^H \mathbf{H}_k \cdot \mathbf{H}_k^{\text{ant}} \mathbf{w}_k|^2}{\sigma^2 \|\mathbf{u}_k\|_2^2 + \sum_{i \neq k, i \in \mathcal{S}} |\mathbf{u}_k^H \mathbf{H}_k \cdot \mathbf{H}_k^{\text{ant}} \mathbf{w}_i|^2} \quad (3)$$

Then achievable rate of each user  $K$  can be represented as:

$$R_k = B \log_2(1 + \text{SINR}_k) \quad (4)$$

where  $B$  represents the bandwidth of the wireless channel. Assume that the transmitter has perfect channel state information (CSI), which is calculated by exploiting the reciprocity concept between downlink and uplink channels, considering that time-division duplex has been used [22]. Saleh-Valenzuela geometric channel model for a small number of clusters has been widely used in the case of small-scale fast fading [23–25]. This channel model is non-selective in both time and frequency, which concentrates only on spatial sides, referencing a frequency-flat fading channel as follows [23–25]:

$$\mathbf{H}_k = \frac{\alpha_k}{\sqrt{C_k L_k}} \sum_{c=1}^{C_k} \sum_{l=1}^{L_k} \xi_{cl}^k \mathbf{a}_r(\theta_{cl}^k, \varphi_{cl}^k) \mathbf{a}_t(\theta_{cl}^{\text{BS}}, \varphi_{cl}^{\text{BS}})^H \quad (5)$$

where  $\alpha_k$  represents the large-scale channel gain reasoned by shadow fading and path loss between user  $k$  and BS, and  $C_k$  represents the main path cluster number from BS to user  $k$ . Each cluster  $C$  is composed of  $L_k$  sub-paths, and there is a complex small-scale fading gain represented as  $\xi_{cl}^k$  for any sub-path  $l$ . This gain has been modelled by complex Gaussian distribution [23, 24]. The vector  $\mathbf{a}_r(\theta_{cl}^k, \varphi_{cl}^k)$  is the vector of receiving response at the azimuth and elevation arrival angles  $(\varphi_{cl}^k, \theta_{cl}^k)$  of sub-path  $l$  in cluster  $c$  at user  $k$ . In addition, the vector  $\mathbf{a}_t(\theta_{cl}^{\text{BS}}, \varphi_{cl}^{\text{BS}})^H$  represents the transmitter steering vector at azimuth and elevation angles of the receiver  $(\varphi_{cl}^k, \theta_{cl}^k)$  of subpath  $l$  in cluster  $c$  at BS. On the other hand, the antenna array channel matrix for user  $k$  can be represented according to [20] as:

$$\mathbf{H}_k^{\text{ant}} = \sum_{c=1}^{C_k} \sum_{l=1}^{L_k} \mathbf{G}(\theta_{cl}^k, \varphi_{cl}^k) \quad (6)$$

where  $\mathbf{G}(\theta_{cl}^k, \varphi_{cl}^k)$  is the diagonal matrix of antenna array gain pattern. This diagonal matrix represents the different active antenna patterns from different arrival angles for each antenna element caused by the mutual coupling, edge, and center effects which are represented as:

$$\mathbf{G}(\theta_{cl}^k, \varphi_{cl}^k) = \text{diag}(\sqrt{\mathbf{g}_1(\theta_{cl}^k, \varphi_{cl}^k)}, \sqrt{\mathbf{g}_2(\theta_{cl}^k, \varphi_{cl}^k)}, \dots, \sqrt{\mathbf{g}_{N_t}(\theta_{cl}^k, \varphi_{cl}^k)}) \quad (7)$$

where  $\mathbf{g}_i(\theta_{cl}^k, \varphi_{cl}^k)$ ,  $\forall i = 1, 2, \dots, N_t$ , represents the gain of element number  $i$  in the array according to the location of user  $k$  ( $\theta_K$  and  $\varphi_K$ ).

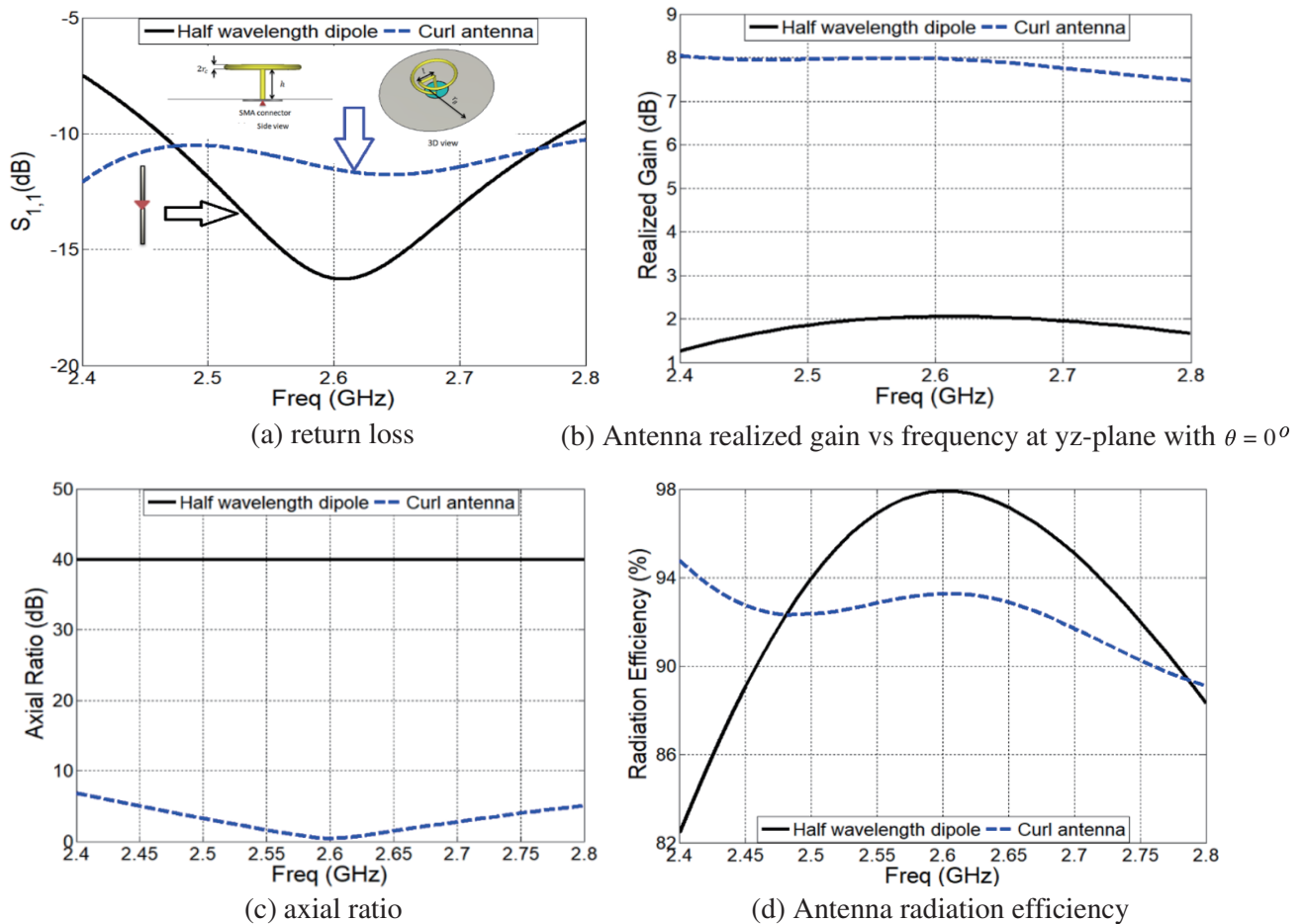
### 3. ANTENNA ARRAY ELEMENTS AND THE ARRAY GEOMETRY CONFIGURATION

In this section, two different antenna array elements are presented. In addition, the conformal array geometries consisting of these elements are configured, and their steering vectors are derived.

### 3.1. Antenna Element

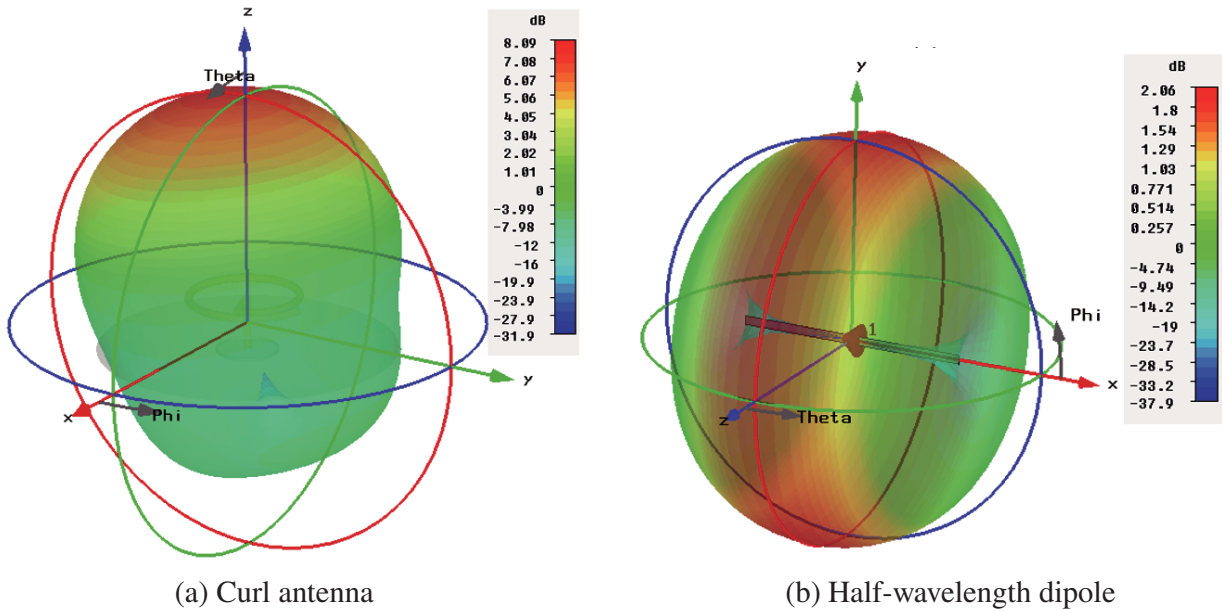
A half-wavelength dipole is the first one where this element has linear polarization and an omnidirectional antenna with a dimension of about  $51.3 \times 2$  mm. The other one is a curl antenna, which is a circularly polarized and directional antenna [26,27]. A curved copper tube with a radius  $r_c = 0.00711\lambda_{2.6\text{GHz}}$  and length  $l = 1.4\lambda_{2.6\text{GHz}}$  has been used to create the curl antenna. This curved copper has been wound into about one turn with radius  $r_w(\phi)$  and mounted above a circular ground plane with radius  $r_g = 0.33\lambda_{2.6\text{GHz}}$  at a height  $h = 0.15\lambda_{2.6\text{GHz}}$ . The curl starts at  $\phi_{st} = 6\pi$  and ends at  $\phi_{en} = 26.3$  rad.

Figure 2 depicts a comparison of these two different elements concerning return loss, antenna gain, axial ratio, and radiation efficiency. Fig. 2(a) depicts that the half-wavelength dipole is a narrow band antenna at 2.6 GHz, but the curl antenna is a wideband antenna. As shown in Fig. 2(b), the curl antenna gain is four times that of the half-wavelength dipole gain. Furthermore, the axial ratio of the curl antenna is less than 3 dB around 2.6 GHz with an approximately 500 MHz band, counter to the half-wavelength dipole which is linearly polarized (Fig. 2(c)). Moreover, the curl antenna is less efficient than a half-wavelength antenna by 5% at 2.6 GHz as depicted in Fig. 2(d).



**Figure 2.** Comparison between half-wavelength dipole and curl antenna with respect to (a) return loss, (b) realized gain, (c) axial ratio, (d) antenna radiation efficiency.

Figure 3 presents the directional antenna, curl antenna and omnidirectional antenna, half-wavelength dipole, 3D radiation patterns at 2.6 GHz.



**Figure 3.** Radiation pattern (a) curl antenna, and (b) half-wavelength dipole at 2.6 GHz.

### 3.2. Antenna Array Geometry

The considered antenna elements have been used as the MIMO array elements in the conformal geometry. The conformal geometry has been chosen based on some previous studies. It is concluded that the CfA geometry achieved much higher system throughput than the uniform planar array, circular array, conical array, and uniform planar circular array.  $M = 32$  identical antenna elements with a 1 mm gap per antenna. In this geometry,  $M = M_{yz}M_x$  where in this geometry the elements are located on a cylindrical style with  $M_{yz} = 8$  and  $M_x = 4$  elements as shown in Fig. 4. In [28], the CfA steering vector

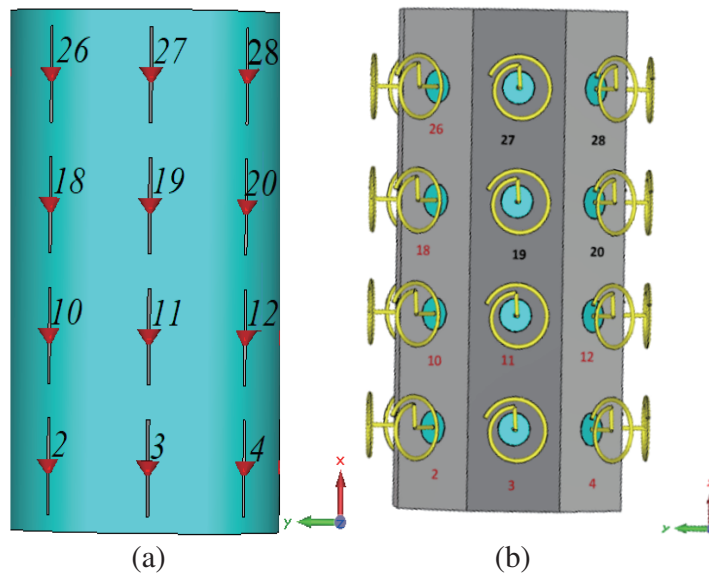


**Figure 4.** Design of conformal array geometry with antenna element (a) half wavelength dipole (b) curl antenna.

can be reformulated as in Eq. (8) in the state of the far-field region.

$$\begin{aligned} \mathbf{a}_{\text{CfA}}(\theta_{\mathbf{k}}, \varphi_{\mathbf{k}}) = & [e^{j\beta(R_{\text{CfA}} \cos 1 - M_{yz} \cos \theta + R_{\text{CfA}} \sin 1 - M_{yz} \sin \theta \sin \varphi + (M_x - 1)(d_\nu/2) \sin \theta \cos \varphi)} \\ & , \dots, e^{j\beta(R_{\text{CfA}} \cos \varphi_{M_{yz}}^{CfA} \cos \theta + R_{\text{CfA}} \sin \varphi_{M_{yz}}^{CfA} \sin \theta \sin \varphi + (M_x + 1 - 2m_x)(d_\nu/2) \sin \theta \cos \varphi)} \\ & , \dots, e^{j\beta(R_{\text{CfA}} \cos M_{yz} - 1 \cos \theta + R_{\text{CfA}} \sin M_{yz} - 1 \sin \theta \sin \varphi + (1 - M_x)(d_\nu/2) \sin \theta \cos \varphi)]^T \end{aligned} \quad (8)$$

$R_{\text{CfA}}$  is the CfA radius while  $d_\nu$  is the vertical plane element spacing.  $d_\nu = d$  in our design.  $\varphi_{m_{yz}}^{CfA} = (2m_{yz} - 1 - M_{yz})\Delta\theta\Delta\varphi/2$  is the angular location of  $m_{yz}^{\text{th}}$  element on  $xy$ -plane, and  $\Delta\theta\Delta\varphi$  is the interelement spacing in the  $yz$ -plane.  $1 \leq m_{yz} \leq M_{yz}$  denotes the antenna element number in the  $yz$ -plane. Index  $1 \leq m_x \leq M_x$  refers to the antenna element number on  $x$ -axis. The two suggested antenna array geometries were created using the CST microwave studio (CST MWS) (see Fig. 4). The estimation of mutual coupling among the array geometries elements can be given from the  $S$ -parameters for both elements in the center and edge of the array, as displayed in Fig. 5. Elements 13 and 14 are chosen for the center and elements 31 and 32 for the edge. The curl CfA has a less mutual coupling effect between its elements than the half-wavelength dipole at 2.6 GHz by approximately 7 dB, because the curl antenna is a directional radiation pattern antenna other than half-wavelength dipole, which is omnidirectional.

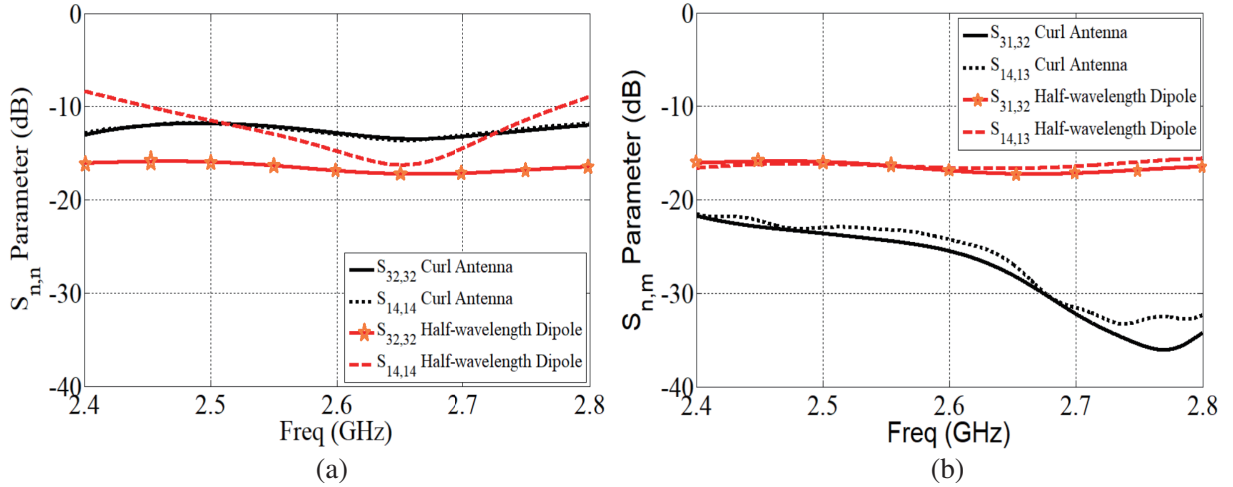


**Figure 5.** The return and insertion loss for conformal array geometries consists of half wavelength dipole and curl antenna elements, (a) return loss, (b) insertion loss.

#### 4. PROBLEM FORMULATION

In this work, the issue of interest is to jointly optimize the beamforming vector of transmission while maximizing the total system rate subject to the QoS requirement of each user. The maximum transmitting power per antenna element and the total transmitted power from the antenna are also considered. The optimization issue can be subedited as:

$$\max_{\mathbf{w}_{\mathbf{k}}, \mathbf{u}_{\mathbf{k}} | \mathbf{k} \in \mathcal{S}} \sum_{k \in \mathcal{J}} U F_k(R_k) \quad (9)$$

subject to

$$\text{SINR}_k \leq \gamma_k \quad \forall k \in \mathcal{S} \quad (9a)$$

$$\sum_{k \in \mathcal{S}} \|\mathbf{w}_{\mathbf{k}}\|_2^2 \leq P_{\max} \quad (9b)$$

$$\left[ \sum_{k \in \mathcal{S}} \mathbf{w}_{\mathbf{k}} \mathbf{w}_{\mathbf{k}}^H \right]_{n_t, n_t} \leq P_{\max}^{n_t} \quad \forall n_t \quad (9c)$$

where  $UF_k(R_k)$  represents the utility function for user  $k$ , and  $\gamma_k$  denotes the user  $k$  target SINR. The quantity  $P_{\max}$  is the maximum power available to transmit from the BS, while  $P_{\max}^{n_t}$  is the maximum power available transmit from the transmitted antenna  $n_t$ . where  $UF_k(R_k) = \log(R_k)$  is the logarithmical utility function used widely in network optimization problems. This utility function has been applied to get acceptable fairness among all users [29].

## 5. BEAMFORMING VECTORS OPTIMIZATION SETTLING

In this research section, the beamforming solution for the formulated optimization problem is provided. Since the formulated optimization problem in Eq. (9) is non-convex, the WMMSE technique is applied to convert the problem into a convex one. After that, the Block Coordinate Descent (BCD) approach is applied to reach a stationary point and decide the receive and transmit beamforming vectors. In this manner, a local optimal settlement can be achieved by tackling the weighted sum MSE minimization issue. That is equivalent to the overall system achievable rate maximization issue in Eq. (9) [9]. For user  $k$  the MSE between the estimated symbol  $\hat{x}_k$  and the transmitted data symbol  $x_k$  at the receiver can be tallied as:

$$\begin{aligned} e_k &= E [|\hat{x}_k - x_k|^2] \\ &= \mathbf{u}_k^H \left( \sigma^2 \mathbf{I} + \sum_{i \in \mathcal{S}} \mathbf{H}_k \cdot \mathbf{H}_k^{\text{ant}} \mathbf{w}_i \mathbf{w}_i^H (\mathbf{H}_k \cdot \mathbf{H}_k^{\text{ant}})^H \right) \mathbf{u}_k - 2 \text{Re}(\mathbf{u}_k^H \mathbf{H}_k \cdot \mathbf{H}_k^{\text{ant}} \mathbf{w}_k) + 1 \end{aligned} \quad (10)$$

where the logarithmic utility function stated in Eq. (9) is increased and strictly concave function, so that the cost function  $Cost_k(\cdot) = -UF_k(-\log_2(\cdot))$  is also strictly concave [9]. So, the considered optimization issue can be converted to the next form:

$$\min_{\mathbf{w}_k, \mathbf{u}_k, t_k | k \in \mathcal{S}} \sum_{k \in \mathcal{J}} (t_k e_k + Cost_k(\delta_k(t_k)) - t_k \delta_k(t_k)) \quad (11)$$

subject to

$$SINR_k \leq \gamma_k, \quad \forall k \in \mathcal{S} \quad (11a)$$

$$\sum_{k \in \mathcal{S}} \|\mathbf{w}_k\|_2^2 \leq P_{\max} \quad (11b)$$

$$\left[ \sum_{k \in \mathcal{S}} \mathbf{w}_k \mathbf{w}_k^H \right]_{n_t, n_t} \leq P_{\max}^{n_t}, \quad \forall n_t \quad (11c)$$

where  $t_k$  represents the user  $k$  weight of MSE, and  $\delta_k(\cdot)$  denotes the map of gradient  $\partial Cost_k(e_k)(\partial e_k)$  inverse. Because of tuning the  $w_k$  phase such that  $u_k^H H_k \cdot H_k^{\text{ant}} w_k$  is positive and real which does not affect the issue (11) [30], the constraints stated in Eq. (11a) can be reformulated as a second-order cone (SOC) constraints as in [30] as see in Eq. (12).

$$\begin{aligned} &\sqrt{\sigma^2 \|\mathbf{u}_k\|_2^2 + \sum_{i \in \mathcal{S}} |\mathbf{u}_k^H \mathbf{H}_k \cdot \mathbf{H}_k^{\text{ant}}|^2} \leq \\ &\sqrt{1 + \frac{1}{\gamma_k} \text{Re}(\mathbf{u}_k^H \mathbf{H}_k \cdot \mathbf{H}_k^{\text{ant}} \mathbf{w}_k)} \quad \forall k \in \mathcal{S} \end{aligned} \quad (12)$$

After that, the reformulated issue can be revised as follows:

$$\min_{\mathbf{w}_k, \mathbf{u}_k, t_k | k \in \mathcal{S}} \sum_{k \in \mathcal{S}} (t_k e_k + Cost_k(\delta_k(t_k)) - t_k \delta_k(t_k)) \quad (13)$$

subject to

$$\sigma^2 \|\mathbf{u}_k\|_2^2 + \sum_{i \in \mathcal{S}} |\mathbf{u}_k^H \mathbf{H}_k \cdot \mathbf{H}_k^{\text{ant}}|^2 \leq \left( 1 + \frac{1}{\gamma_k} \right) |\mathbf{u}_k^H \mathbf{H}_k \cdot \mathbf{H}_k^{\text{ant}} \mathbf{w}_k|^2 \quad \forall k \in \mathcal{S} \quad (13a)$$

$$\mathbf{u}_k^H \mathbf{H}_k \cdot \mathbf{H}_k^{\text{ant}} \mathbf{w}_k \geq 0 \quad \forall k \in \mathcal{S} \quad (13b)$$

$$\mathbf{Im}(\mathbf{u}_k^H \mathbf{H}_k \cdot \mathbf{H}_k^{\text{ant}} \mathbf{w}_k) = 0 \quad \forall k \in \mathcal{S} \quad (13c)$$

$$\sum_{k \in \mathcal{S}} \|\mathbf{w}_k\|_2^2 \leq \mathbf{P}_{\max} \quad (13d)$$

$$\left[ \sum_{k \in \mathcal{S}} \mathbf{w}_k \mathbf{w}_k^H \right]_{n_t, n_t} \leq P_{\max}^{n_t}, \quad \forall n_t \quad (13e)$$

The optimization problem in Eq. ((13)) is convex regarding all variables of individual optimization,  $w_k$ ,  $u_k$ , and  $t_k$  whereas saving other variables settles. Then, the BCD approach [14] has been used to settle Eq. ((13)) through the following procedures:

- (1) The optimal  $u_k$  under constant  $w_k$  and  $t_k$  has been acquired by applying the MMSE approach receiver as:

$$\mathbf{u}_k^* = \left( \sigma^2 \mathbf{I} + \sum_{i \in \mathcal{S}} \mathbf{H}_k \cdot \mathbf{H}_k^{\text{ant}} \mathbf{w}_i \mathbf{w}_i^H (\mathbf{H}_k \cdot \mathbf{H}_k^{\text{ant}})^H \right)^{-1} \mathbf{H}_k \cdot \mathbf{H}_k^{\text{ant}} \mathbf{w}_k \quad (14)$$

- (2) For constant  $u_k$  and  $w_k$ , the optimal value of the MSE weight  $t_k$  is calculated by

$$\begin{aligned} t_k^* &= \frac{\partial \text{Cost}_k(e_k)}{\partial e_k} \\ &= \frac{e_k^{-1}}{\log_2 e_k} \quad \forall k \in \mathcal{S} \end{aligned} \quad (15)$$

- (3) For specific  $u_k$  and  $t_k$ , the optimal transmitted beamformer  $w_k$  can be tallied by settling the following quadratic programming constrained issue:

$$\min_{\mathbf{w}_k | k \in \mathcal{S}} \sum_{k \in \mathcal{S}} \mathbf{w}_k^H \left( \sum_{i \in \mathcal{S}} t_i (\mathbf{H}_i \cdot \mathbf{H}_i^{\text{ant}})^H \mathbf{u}_i \mathbf{u}_i^H \mathbf{H}_i \cdot \mathbf{H}_i^{\text{ant}} \right) \mathbf{w}_k - 2 \sum_{k \in \mathcal{S}} t_k \text{Re}(\mathbf{u}_k^H \mathbf{H}_k \cdot \mathbf{H}_k^{\text{ant}} \mathbf{w}_k) \quad (16)$$

subject to: same Eq. (13) constraints

Because of the function's convex quadratic property in Eq. (16), the constraints in Eqs. (13a)–(13c) are convex SOC. Furthermore, Eqs. (13d) and (13e) are convex quadratic constraints. So the issue in Eq. (16) represents convex optimization issue with zero duality gap between between dual optimum and primal optimum [31]. Thus, closed form settling can be occupied by applying the Lagrange multipliers approach. Let  $\mu = \mu_1, \mu_2, \dots, \mu_K$  and  $\rho = \rho_1, \rho_2, \dots, \rho_{n_t}$  represent vectors of Lagrange multiplier correlated with constraints in Eqs. (13a) and (13e), respectively. Also,  $\rho_o$  denotes the multiplier correlated with the constraint in Eq. (13d). After that, the problem's Eq. (16) Lagrangian function is presented as in Eq. (17) below.

$$\begin{aligned} \mathcal{L}(\mathbf{w}_k, \mu, \rho, \rho_o) &= \sum_{k \in \mathcal{S}} \mathbf{w}_k^H \left( \sum_{i \in \mathcal{S}} t_i (\mathbf{H}_i \cdot \mathbf{H}_i^{\text{ant}})^H \mathbf{u}_i \mathbf{u}_i^H \mathbf{H}_i \cdot \mathbf{H}_i^{\text{ant}} \right) \mathbf{w}_k - 2 \sum_{k \in \mathcal{S}} t_k \text{Re}(\mathbf{u}_k^H \mathbf{H}_k \cdot \mathbf{H}_k^{\text{ant}} \mathbf{w}_k) \\ &\quad - \sum_{k \in \mathcal{S}} \left( \mathbf{w}_k^H (\gamma_k^{-1} \mu_k (\mathbf{H}_k \cdot \mathbf{H}_k^{\text{ant}})^H \mathbf{u}_k \mathbf{u}_k^H \mathbf{H}_k \cdot \mathbf{H}_k^{\text{ant}} \right. \\ &\quad \left. - \sum_{i \neq k, i \in \mathcal{S}} \mu_i (\mathbf{H}_i \cdot \mathbf{H}_i^{\text{ant}})^H \mathbf{u}_i \mathbf{u}_i^H \mathbf{H}_i \cdot \mathbf{H}_i^{\text{ant}} \right) \mathbf{w}_k - \mu_k \sigma^2 \|\mathbf{u}_k\|_2^2 \\ &\quad + \rho_o \left( \sum_{k \in \mathcal{S}} \mathbf{w}_k^H \mathbf{w}_k - \mathbf{P}_{\max} \right) + \sum_{k \in \mathcal{S}} \mathbf{w}_k^H \psi \mathbf{w}_k - \sum_{n_t=1}^{n_t} \rho_{n_t} \mathbf{P}_{\max}^{n_t} \end{aligned} \quad (17)$$

$$\psi = \text{diag}(\rho_1, \rho_2, \dots, \rho_{n_t}) \quad (18)$$

By applying the optimal condition of first-order [31], the optimal transmitted beamforming vector  $\mathbf{w}_k$  can be calculated by Eq. (19) below. Furthermore, the following equations enable us to calculate the optimum multipliers, by applying a gradient method.

$$\mathbf{w}_k^* = t_k \left( \sum_{k \in \mathcal{S}} t_k (\mathbf{H}_k \cdot \mathbf{H}_k^{\text{ant}})^{\mathbf{H}} \mathbf{u}_k \mathbf{u}_k^{\mathbf{H}} \mathbf{H}_k \cdot \mathbf{H}_k^{\text{ant}} - \gamma_k^{-1} \mu_k \mathbf{H}_k^{\mathbf{H}} \mathbf{u}_k \mathbf{u}_k^{\mathbf{H}} \mathbf{H}_k \cdot \mathbf{H}_k^{\text{ant}} + \sum_{i \neq k, i \in \mathcal{S}} \mu_i (\mathbf{H}_i \cdot \mathbf{H}_i^{\text{ant}})^{\mathbf{H}} \mathbf{u}_i \mathbf{u}_i^{\mathbf{H}} \mathbf{H}_i \cdot \mathbf{H}_i^{\text{ant}} + \psi + \rho_o \mathbf{I} \right)^{-1} (\mathbf{H}_k \cdot \mathbf{H}_k^{\text{ant}})^{\mathbf{H}} \mathbf{u}_k \quad (19)$$

$$\mu_k^{(t+1)} = \left[ \mu_k^t + b^{(t)} \left( \sigma^2 \|\mathbf{u}_k\|_2^2 + \sum_{k \in \mathcal{S}} |\mathbf{u}_k^{\mathbf{H}} \mathbf{H}_k \cdot \mathbf{H}_k^{\text{ant}} \mathbf{w}_k|^2 \right) - \left( 1 + \frac{1}{\gamma_k} |\mathbf{u}_k^{\mathbf{H}} \mathbf{H}_k \cdot \mathbf{H}_k^{\text{ant}} \mathbf{w}_k|^2 \right) \right]^+ \quad (20)$$

$$\rho_o^{(t+1)} = \left[ \rho_o^t + b^{(t)} \left( \sum_{k \in \mathcal{S}} \|\mathbf{w}_k\|_2^2 - \mathbf{P}_{\max} \right) \right]^+ \quad (21)$$

$$\rho_{n_t}^{(t+1)} = \left[ \rho_{n_t}^t + b^{(t)} \left( \left[ \sum_{k \in \mathcal{S}} \mathbf{w}_k \mathbf{w}_k^{\mathbf{H}} \right]_{n_t, n_t} - P_{\max}^{n_t} \right) \right]^+ \quad (22)$$

where  $t$  is the index of iteration, and  $b(t)$  represents the step size.  $[\cdot]^+$  denotes a projection on the set of  $\mathbb{R}^+$ . The algorithm (1) summarizes the solution steps of WMMSE-based. Note that  $g$  represents a small constant applied for convergence problem, and  $t_{\max}$  represents the maximum iterations number.  $\mathcal{O}(TKN_t)$  is Algorithm (1) complexity of the computational [22], where  $T$  denotes the iteration number.

---

### Algorithm 1

---

**Initialize:**  $t = 0$ ,  $g = t_{\max}$ ,  $\rho_0^{(0)} = 0$ ,  $\rho_{n_t}^{(0)} = 0$ ,  $\forall n_t$ ,  $c = 0$ ,  $t_k^{(0)} = 0$ ,  $R_k^{(0)} = 0$ ,  $\mathbf{w}_k^{(0)} > \forall \mathbf{k} \in \mathcal{S}$ .

Calculate the gain matrix from Eq. (7) after uniformly antenna array feeding.

Calculate the antenna channel matrix from Eq. (6).

Calculate the channel matrix from Eq. (5).

**Repeat:**

1: Run the CST-MWS through the MATLAB program;

2: Feed the designed antenna array elements on CST MWS by  $\mathbf{w}_k^{(t)}$ ;

3: Extract the diagonal matrix array gain pattern as in Eq. (7) from the CST-MWS;

4: Stop the CST-MWS through the MATLAB program;

5: Calculate the  $\mathbf{H}_k^{\text{ant}}$  from Eq. (6) ;

6: Calculate the channel matrix  $\mathbf{H}_k$  from Eq. (5);

7: Compute the optimal receive beamformer  $\mathbf{u}_k^{(t+1)}$  from Eq. (16) under fixed  $\mathbf{w}_k^{(t)}$  and  $t_k^{(t)}$ ;

8: Fix  $\mathbf{u}_k^{(t+1)}$  and  $\mathbf{w}_k^{(t)}$ , obtain the optimal MSE weight  $t_k^{(t+1)}$  by Eq. (15);

9: Update  $\mu_k^{(t)}$ ,  $\rho_o^{(t+1)}$  and  $\rho_{n_t}^{(t+1)}$  according to Eqs. (20), (21), (22);

10: Obtain the optimal transmit beamformer  $\mathbf{w}_k^{(t+1)}$  by using Eq. (19) under fixed  $\mathbf{u}_k^{(t+1)}$  and  $t_k^{(t+1)}$ ;

11: Compute the achievable rate  $R_k^{(t+1)}$  by using Eq. (3) using  $\mathbf{u}_k^{(t+1)}$  and  $\mathbf{w}_k^{(t+1)}$ ;

12: Let  $t = t + 1$ ;

**Until**  $\left| \sum_{k \in \mathcal{S}} \log(R_k^{(t)}) - \sum_{k \in \mathcal{S}} \log(R_k^{(t-1)}) \right| \leq g$ , or  $t = t_{\max}$

---

## 6. NUMERICAL RESULTS

In this section, the execution of the suggested beamforming settling is studied and numerically analyzed. There are two metrics exploited in this research. The first one is system throughput, and the second one is system power consumption. System throughput is calculated by summing all users  $k \in \mathcal{S}$  achievable rate as:

$$\text{System Throughput} = \sum_{k \in \mathcal{S}} R_k \quad (23)$$

where the user  $k$  achievable rate  $R_k$  has been obtained using Eq. (4) as part of the optimized beamforming vector  $\mathbf{w}_k$ . The single BS found at the center of a circular cell has a radius 1 km which is considered to serve  $k$  users, where the users have been uniformly distributed over the cell coverage area. Also, constraints on the rate of the users have been distributed uniformly in the range of 180 to 360 kbps, so the users' equivalent target SINR values  $\gamma_k, \forall k \in \mathcal{S}$  have been distributed from 1 to 3 dB according to Eq. (5) [18]. Then, the path loss is calculated in dB [31] as:

$$PL(d_k) = 40.74 + 10 \times n \log_{10}(d_k) \quad (24)$$

where  $d_k$  represents the distance between user  $k$  and the BS in meters.  $n = 3$  for non-line-of-sight (NLOS) paths; however,  $n = 2$  for line-of-sight (LOS) paths [31] where  $n$  denotes the exponent of the path loss. The standard deviation of the shadowing is 6.8 dB and 4.1 dB for NLOS and LOS [31], respectively. Assume that the complex small-scale fading gain  $\xi_{cl}^k$  is distributed as  $CN(0, 1)$ . All users are assumed to have  $C_k = 1$ , where the arrival azimuth angle  $\phi_{cl}^k$  and departure azimuth angle  $\phi_{cl}^{BS}$  of each sub-path  $l$  in this main cluster path can be produced as wrapped Gaussians near the mean cluster angles with a standard deviation of  $30^\circ$ . However, the arrival elevation angle  $\theta_{cl}^k$  and the departure elevation angle  $\theta_{cl}^{BS}$  have been suggested to have a standard deviation of  $5^\circ$  near the mean cluster angles. The other used parameters in this research are stated in Table 1. The initial transmitted beamforming vector  $\mathbf{w}_k(\mathbf{0})$  has been determined by applying the right singular matrices initialization approach. Additionally, the acquired numerical results have been completed by averaging 500 runs, where each run includes five realizations of small-scale channels.

**Table 1.** The values of the simulation parameters.

Parameter	Value
$k$	24
$N_t$	32
$\sigma^2$	-174 dBm/Hz
$B$	180 Hz
$L_k$	10
$f$	2.6 GHz
$P_{\max}$	43 dBm
$g$	0.001
$t_{\max}$	200
$N_r$	1

The gain matrix has been directly extracted from the CST MWS. Therefore, the first step in our optimization beamforming algorithm is the design of the array geometry on the CST. After that, the CST and MATLAB link have been coded to extract the gain matrix based on antenna array feeding through the calculated optimum transmitting beamforming weights through MATLAB as displayed in Fig. 6.

Considering isotropic elements as usually proposed in previous work, it is clear that the system throughput of our proposed model with a practical antenna is larger than the isotropic one provided in

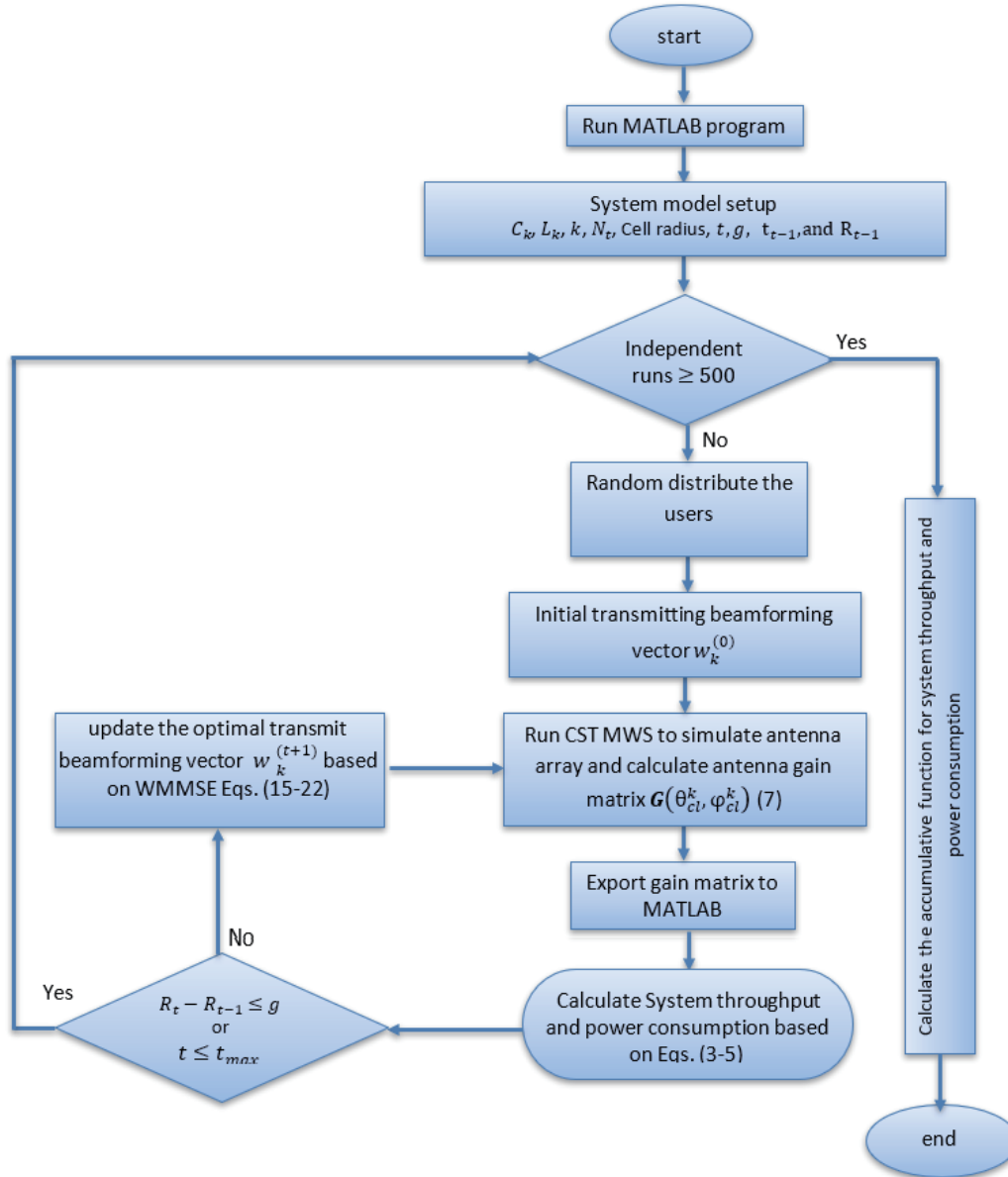


**Figure 6.** The proposed beamforming optimization algorithm flowchart.

the previous model by 1.8 Mbps, in addition to its lower power consumption than the isotropic one, as shown in Fig. 7.

For a fair comparison between our proposed beamforming solution and the previous beamforming solution in [18], the conformal array geometry with half-wavelength dipole elements has been explored in both solutions. As seen in Fig. 8, the proposed approach has a higher system throughput than the solution in [18]. For example, there is an 80% probability of achieving system throughput of less than or equal to 3.5 Mbps using the proposed beamforming optimization solution. On the other hand, the algorithm in [18] can achieve only less than or equal to 3.1 Mbps system throughput for the same probability.

Moreover, the suggested solution has the same power consumption as the solution in [18] which is displayed in Fig. 9. The convergence of the optimization solution in the proposed algorithm is also displayed in Fig. 10.

Another antenna array element has been presented to study the impact of the array gain on the system performance. This element must be different from the half-wavelength dipole. So, the curl

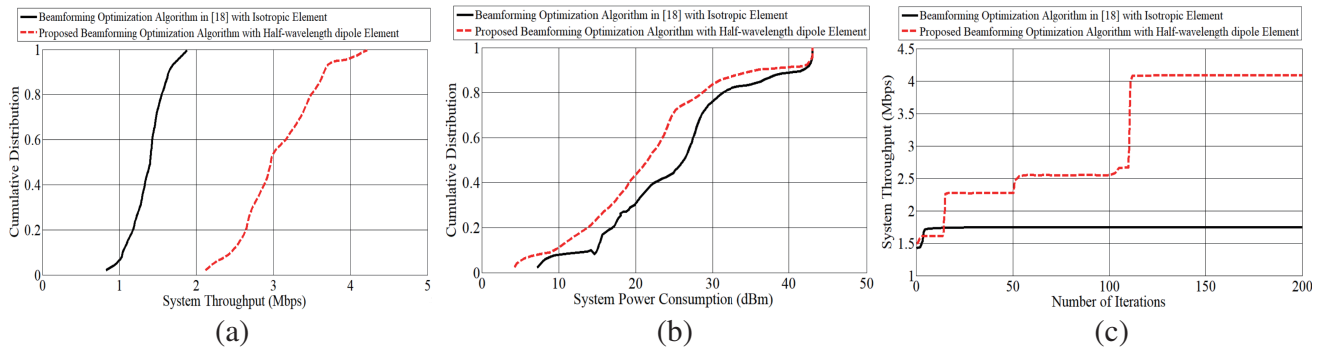


**Figure 7.** Effect of practical antenna array gain on system performance when CfA geometry (a) cumulative distribution functions of system throughput, (b) cumulative distribution functions of system power consumption, (c) number of iterations VS system throughput.

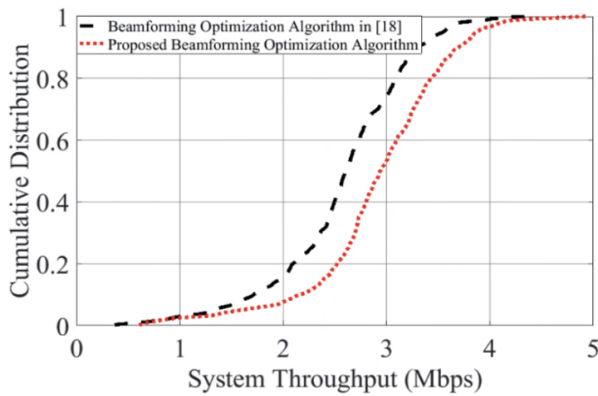


**Figure 8.** Comparison between the suggested settling and algorithm in [18] with half wavelength dipole CfA geometry at BS with respect to the system throughput cumulative distribution function.

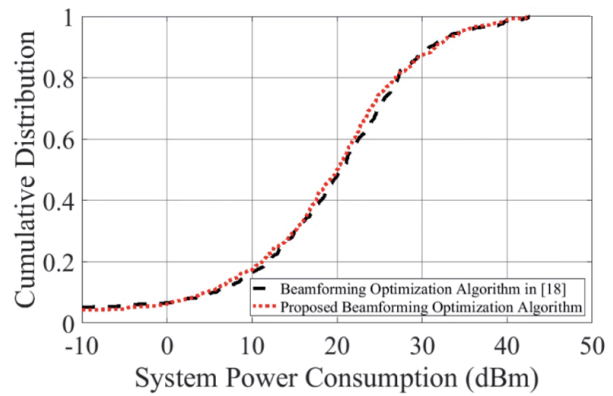


**Figure 9.** Comparison between the suggested settling and algorithm in [18] with half wavelength dipole CfA geometry at the BS with respect to Cumulative distribution function of system power consumption.

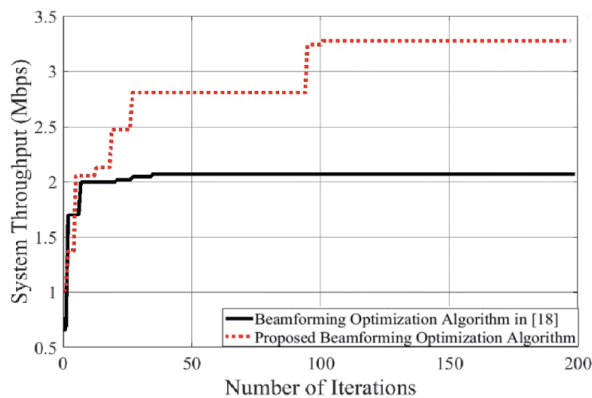


**Figure 10.** Convergence of the suggested settling and algorithm in [18].

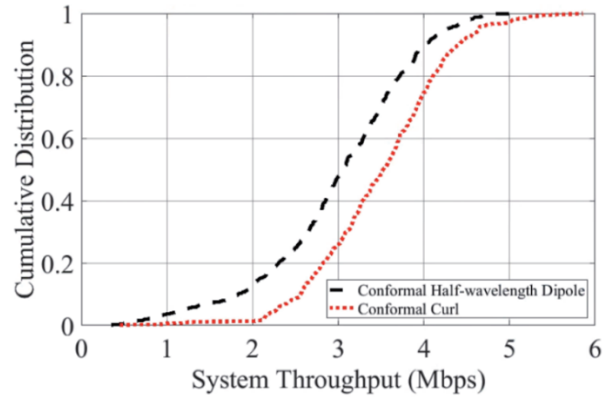


**Figure 11.** Comparison between CfA with half wavelength dipole and curl antenna elements with respect to system throughput cumulative distribution functions.

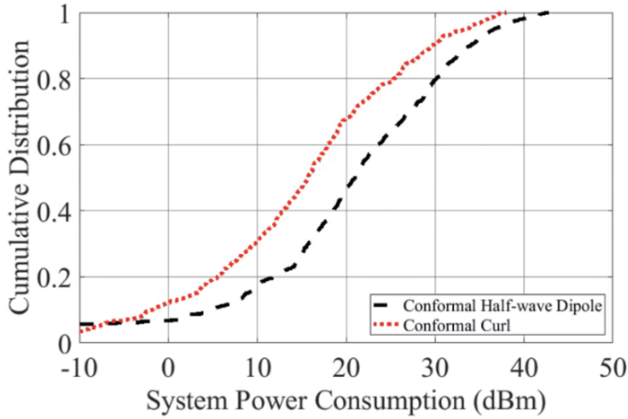


**Figure 12.** Comparison between CfA with half wavelength dipole and curl antenna elements with respect to power consumption cumulative distribution functions.

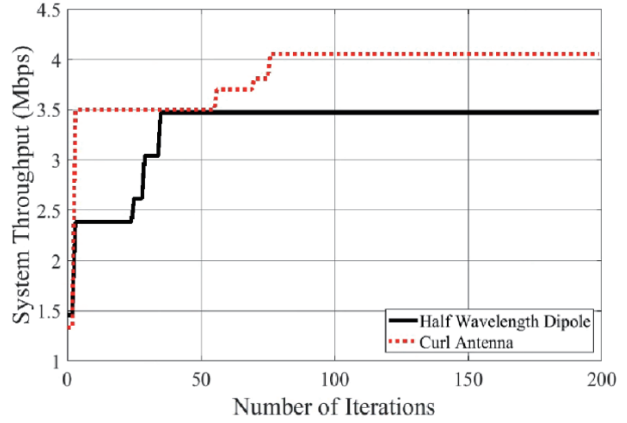


**Figure 13.** Comparison between CfA with half wavelength dipole and curl antenna elements with respect to iterations number VS system throughput.

antenna has been used where the curl antenna has a larger gain than a half-wavelength dipole by four times. In addition, the curl antenna is circularly polarized, unlike the half-wavelength dipole, which is linearly polarized. Finally, the curl antenna is a directional antenna, but the half-wavelength dipole is an omnidirectional one. Fig. 11 depicts a rapprochement between the system execution of the conformal half-wavelength dipole array and the octagonal prism curl antenna array. The figure shows that the overall system throughput of the conformal half-wavelength dipole array is less than the octagonal prism curl antenna array. This can be explained by the higher gain of the curl antenna than the half-wavelength dipole. As displayed in Fig. 11, the half wave-length dipole CfA has an 80% probability to achieve system throughput less than or equal to 3.65Mbps. However, the curl CfA can achieve only less than or equal to 4.1Mbps of system throughput for the same probability. Furthermore, CfA curl has low power consumption compared to the CfA half-wavelength dipole, as displayed in Fig. 12. Fig. 13 shows the algorithm convergence in which reasonable iteration numbers are needed to reach the optimum transmitting beamforming vector.

As depicted above, the curl antenna has an advantage over a half-wavelength dipole in that it is a circularly polarized antenna, so this feature can be utilized to decrease the interference between users and maximize the overall system throughput. To show that, we consider four different transmission

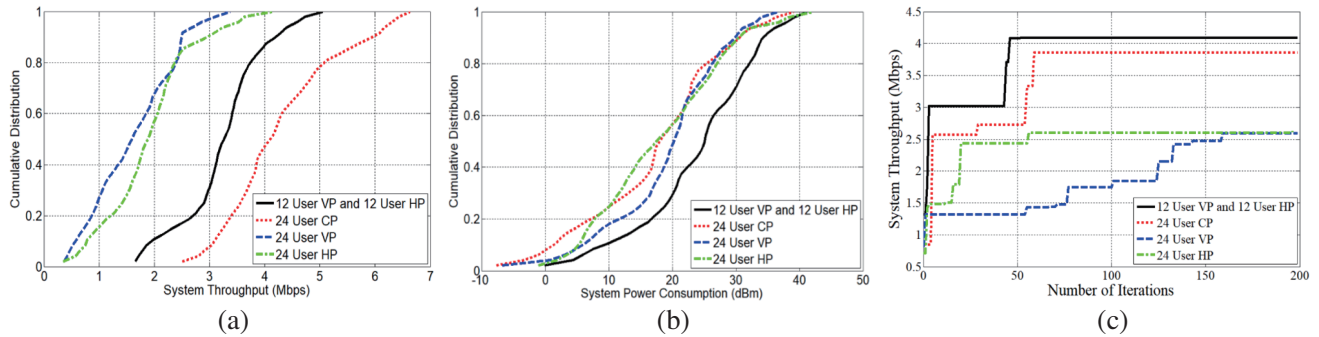


**Figure 14.** Comparison between CfA curl antenna geometry if all users connected circularly polarized (CP) or half of them connected vertical polarized (VP) and others connected horizontal polarized (HP) with respect to (a) system throughput cumulative distribution functions, system power consumption cumulative distribution functions, (c) iterations number VS system throughput.

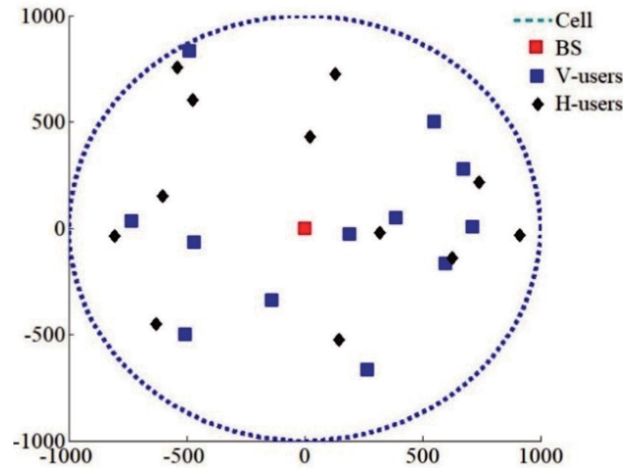


**Figure 15.** Locations of 24 user inside the cell in case of divided them 12 users vertical and 12 user horizontal.

models among the users and the MIMO BS. In the first model, the antenna array channel matrix for each  $k$  uses the circularly polarized (CP) gain matrix. On the other hand, in the second model, we divide the users into halves using the vertically polarized (VP) gain matrix. The second half of users will use the horizontally polarized (HP) gain matrix in the channel matrix of an antenna array. Models three and four require that all users use either a vertically or horizontally gain matrix in the channel model calculations. From Fig. 14, it can be concluded that the division model has 1 Mbps system throughput more than model one where the user uses the total gain. Moreover, it consumed more power with a maximum number of iterations than the first model. On the other hand, the division model enables us to raise the system capacity with a slight minimization in the overall system throughput.

Figure 15 shows the methodology that has been followed to divide users in model 2. If the users are very close to each other, we select one user to receive vertically and the other one to receive horizontally to decrease the interference between them.

## 7. CONCLUSIONS

In this research, the massive MIMO channel model is modified to consider the practical variation in antenna gain in the beamforming solution. Furthermore, the issue of beamforming optimization with maximizing the overall system achievable rate in a multiuser downlink MIMO system, subject to the needed QoS for each user, the transmitted power from each antenna, and total BS transmitted power constraints, is considered. To handle this non-convex issue, a WMMSE-based approach is suggested, where the relationship between the overall system achievable rate maximization issue and the weighted sum MSE minimization issue is exploited, to convert this issue into a convex optimization issue. Then the receiving and transmitting beamforming vectors are calculated using the BCD approach, where each time in array feeding, the weights are used to calculate the practical array gain. To get beamforming towards the required users with high directivity, narrow beamwidth, and small side lobe level, the CfA geometry with half-wavelength dipole elements is proposed, and its steering vector is designed. The numerical and simulation display that the CfA using the suggested settling can outperform the CfA with another comparable algorithm concerning system power consumption and system throughput. However, another suggested antenna array element, the curl antenna, has been designed to cover 2.6 GHz. This curl antenna provides a higher gain than a half-wavelength dipole. So the curl array has proved to have better performance than the half-wavelength dipole, with respect to system throughput and system power consumption. Furthermore, this curl antenna, a circularly polarized antenna, can be exploited to decrease the interference and increase the overall system throughput. Therefore, the effect of various criteria of user connection with the BS is studied and evaluated.

## ACKNOWLEDGMENT

The authors would like to express their gratitude to the National Telecommunication Regulatory Authority (NTRA) in Egypt for their support.

## REFERENCES

1. Marzetta, T. L., "Noncooperative cellular wireless with unlimited numbers of base station antennas," *IEEE Trans. Wireless Commun.*, Vol. 9, No. 11, 3590–3600, 2010.
2. Larsson, E. G., F. Tufvesson, O. Edfors, and T. L. Marzetta, "Massive MIMO for next generation wireless systems," *IEEE Commun. Magazine*, Vol. 52, No. 2, 186–195, 2014.
3. Andrews, J. G., S. Buzzi, W. Choi, S. V. Hanly, A. Lozano, A. C. K. Soong, and J. C. Zhang, "What will 5G be?" *IEEE J. Sel. Areas Commun.*, Vol. 32, No. 6, 1065–1082, 2014.
4. Larsson, E. G. and L. V. der Perre, "Massive MIMO for 5G," *IEEE 5G Tech Focus*, Vol. 1, No. 1, 2017.
5. Arunitha, A., T. Gunasekaran, and N. S. Kumar, "Adaptive beam forming algorithms for MIMO antenna," *J. Innov. Technol. Explor. Eng.*, Vol. 14, No. 8, 9–12, 2015.
6. Han, S., I. Chih-Lin, Z. Xu, and C. Rowell, "Large-scale antenna systems with hybrid analog and digital beamforming for millimeter wave 5G," *IEEE Communications Magazine*, Vol. 53, No. 1, 186–194, 2015.
7. Vook, F. W., A. Ghosh, and T. A. Thomas, "MIMO and beamforming solutions for 5G technology," *2014 IEEE MTT-S International Microwave Symposium (IMS2014)*, Jun. 1, 2014.
8. Yang, B., Z. Yu, J. Lan, R. Zhang, J. Zhou, and W. Hong, "Digital beamforming-based massive MIMO transceiver for 5G millimeter-wave communications," *IEEE Transactions on Microwave Theory and Technique*, Vol. 66, No. 7, 3403–3418, 2018.
9. Shi, Q., M. Razaviyayn, Z. Q. Luo, et al., "An iteratively weighted MMSE approach to distributed sum-utility maximization for a MIMO interfering broadcast channel," *IEEE Trans. Signal. Process.*, Vol. 59, No. 9, 4331–4340, 2011.
10. Shi, Y., J. Zhang, and K. B. Letaief, "Group sparse beamforming for green cloud-RAN," *IEEE Trans. Wirel. Commun.*, Vol. 13, No. 5, 2809–2823, 2014.
11. Dai, B. and W. Yu, "Sparse beamforming and user-centric clustering for downlink cloud radio access network," *IEEE Access*, Vol. 2, 1326–1339, 2014.
12. Luo, S., R. Zhang, and T. J. Lim, "Downlink and uplink energy minimization through user association and beamforming in CRAN," *IEEE Trans. Wirel. Commun.*, Vol. 14, No. 1, 494–508, 2015.
13. Cumanan, K., Z. Ding, et al., "Rahulamathavan. Robust MMSE beamforming for multiantenna relay networks," *IEEE Trans. Veh. Technol.*, Vol. 66, No. 5, 3900–3912, 2018.
14. Wang, K., K. Yang, and C. Magurawalage, "Joint energy minimization and resource allocation in C-RAN with mobile cloud," *IEEE Trans. Cloud Comput.*, Vol. 6, No. 3, 760–770, 2017.
15. Li, H., Z. Wang, and H. Wang, "Joint user association and power allocation for massive MIMO hetnets with imperfect CSI," *Signal Processing*, Vol. 173, 2020.
16. Mai, R., D. H. N. Nguyen, and T. Le-Ngoc, "MMSE hybrid precoder design for millimeter-wave massive MIMO systems," *2016 IEEE Wireless Communications and Networking Conf.*, 1–6, Doha, Apr. 2016.
17. Nasser, S., M. R. Nakhai, and T. A. Le, "Chance constrained robust downlink beamforming in multicell networks," *IEEE Trans. Mob. Comput.*, Vol. 15, No. 11, 2682–2691, 2016.
18. Abdelhakam, M. M., M. M. Elmesalawy, K. R. Mahmoud, and I. I. Brahim, "Efficient WMMSE beamforming for 5G mmWave cellular networks exploiting the effect of antenna array geometries," *IET Communications*, Vol. 122, 169–178, 2017.

19. Li, H., J. Cheng, Z. Wang, and H. Wang, "Joint antenna selection and power allocation for an energy-efficient massive MIMO system," *IEEE Wireless Commun. Letters*, Vol. 8, No. 1, 257–260, 2019.
20. Chen, C.-M., V. Volski, L. V. D. Perre, G. A. E. Vandenbosch, and S. Pollin, "Finite large antenna arrays for massive MIMO: Characterization and system impact," *IEEE Transactions on Antennas and Propagation*, Vol. 65, No. 12, 6712–6720, 2017.
21. Marinovic, T., A. Farsaei, R. Maaskant, A. L. Lavieja, M. N. Johansson, U. Gustavsson, and G. A. E. Vandenbosch, "Effect of antenna array element separation on capacity of MIMO systems including mutual coupling," *2019 IEEE International Symposium on Antennas and Propagation and USNC-URSI Radio Science Meeting*, 415–416, 2019.
22. Huang, X., G. Xue, R. Yu, et al., "Joint scheduling and beamforming coordination in cloud radio access networks with QoS guarantees," *IEEE Trans. Veh. Technol.*, Vol. 65, No. 7, 5449–5460, 2016.
23. Kulkarni, M. N., A. Ghosh, and J. G. Andrews, "A comparison of MIMO techniques in downlink millimeter wave cellular networks with hybrid beamforming," *IEEE Trans. Commun.*, Vol. 64, No. 5, 1952–1967, 2016.
24. Xia, P., R. W. Heath, and N. Gonzalez-Prelcic, "Robust analog precoding designs for millimeter wave MIMO transceivers with frequency and time division duplexing," *IEEE Trans. Commun.*, Vol. 64, No. 11, 4622–4634, 2016.
25. Andrews, J. G., T. Bai, M. N. Kulkarni, et al., "Modeling and analyzing millimeter wave cellular systems," *IEEE Trans. Commun.*, Vol. 65, No. 1, 403–430, 2017.
26. Nakano, H., S. Okuzawa, K. Ohishi, H. Mimaki, and J. Yamauchi, "A curl antenna," *IEEE Transactions on Antennas and Propagation*, Vol. 41, No. 11, 1570–1575, 1993.
27. Zainud-Deen, S. H., K. R. Mahmoud, and M. El-Adawy, "Sabry MM Ibrahim. Design of Yagi-Uda antenna and electromagnetically coupled curl antenna using particle swarm optimization algorithm," *Proceedings of the Twenty-Second National Radio Science Conference, NRSC*, 115–124, 2005.
28. Noordin, N. H., V. Zuniga, A. O. El-Rayis, N. Haridas, A. T. Erdogan, and T. Arslan, "Uniform circular arrays for phased array antenna," *Loughborough Antennas and Propagation Conference*, Loughborough, 2011.
29. Tang, J., W. P. Tay, and T. Q. S. Quek, "Cross-layer resource allocation with elastic service scaling in cloud radio access network," *IEEE Trans. Wirel. Commun.*, Vol. 14, No. 9, 5068–5081, 2015.
30. Nasir, A. A., H. D. Tuan, D. T. Ngo, et al., "Path-following algorithms for beamforming and signal splitting in RF energy harvesting networks," *IEEE Commun. Lett.*, Vol. 20, No. 8, 1687–1690, 2016.
31. Boyd, S. and L. Vandenberghe, *Convex Optimization*, Cambridge University Press, Cambridge, UK, 2004.